

Chapter 2

A Neuromechanical Model of Spinal Control of Locomotion

Sergey N. Markin, Alexander N. Klishko, Natalia A. Shevtsova,
Michel A. Lemay, Boris I. Prilutsky and Ilya A. Rybak

Abstract We have developed a neuromechanical computational model of cat hindlimb locomotion controlled by spinal central pattern generators (CPGs, one per hindlimb) and motion-dependent afferent feedback. Each CPG represents an extension of previously developed two-level model (Rybak et al. J Physiol 577:617–639, 2006a, J Physiol 577:641–658, 2006b) and includes a half-center rhythm generator (RG), generating the locomotor rhythm, and a pattern formation (PF) network operating under control of RG and managing the synergetic activity of different hindlimb motoneuronal pools. The basic two-level CPG model was extended by incorporating additional neural circuits allowing the CPG to generate the complex activity patterns of motoneurons controlling proximal two-joint muscles (Shevtsova et al., Chap. 5, Neuromechanical modeling of posture and locomotion, Springer, New York, 2015). The spinal cord circuitry in the model includes reflex circuits mediating reciprocal inhibition between flexor and extensor motoneurons and disynaptic excitation of extensor motoneurons by load-sensitive afferents. The hindlimbs and trunk were modeled as a 2D system of rigid segments driven by Hill-type muscle actuators with force-length-velocity dependent properties. The musculoskeletal model has been tuned to reproduce the mechanics of locomotion; as a result, the computed motion-dependent activity of muscle group Ia, Ib, and II afferents and the paw-pad cutaneous afferents matched well the cat in vivo afferent recordings reported in the literature (Prilutsky et al., Chap. 10, Neuromechanical modeling of posture and locomotion, Springer, New York, 2015). In the neuromechanical model, the CPG operation is adjusted by afferent feedback from the moving hindlimbs. The

S. N. Markin (✉) · N. A. Shevtsova · I. A. Rybak
Department of Neurobiology and Anatomy, Drexel University College of Medicine,
2900 W. Queen Lane, Philadelphia, PA 19129, USA
e-mail: smarkin@drexelmed.edu

A. N. Klishko · B. I. Prilutsky
School of Applied Physiology, Center for Human Movement Studies,
Georgia Institute of Technology, 555 14th Street NW, Atlanta, GA 30332, USA
e-mail: aklishko3@gatech.edu

M. A. Lemay
Department of Bioengineering, Temple University, 1947 N 12th St, Philadelphia, PA 19122, USA

© Springer Science+Business Media New York 2016

B. I. Prilutsky, D. H. Edwards (eds.), *Neuromechanical Modeling of Posture and Locomotion*, Springer Series in Computational Neuroscience,
DOI 10.1007/978-1-4939-3267-2_2

model demonstrates stable locomotion with realistic mechanical characteristics and exhibits realistic patterns of muscle activity. The model can be used as a testbed to study spinal control of locomotion in various normal and pathological conditions.

Keywords Neuromechanical modeling · Central pattern generator · Afferent feedback · Locomotion · Cat

2.1 Introduction

The mammalian spinal cord contains neural circuits that can generate a basic locomotor rhythm in the absence of rhythmic input from higher brain centers and peripheral afferent feedback (Brown 1911; Grillner 1981; Pearson 1995; Rossignol 1996; Orlovsky et al. 1999). These circuits are commonly referred to as the *central pattern generator* (CPG). During normal locomotion, however, the spinal CPG operates under the control of afferent feedback and descending signals from supraspinal centers, which both modify the locomotor pattern generated by the CPG and adjust it to the particular motor task and external environment (Conway et al. 1987; Gossard et al. 1994; Guertin et al. 1995; McCrea et al. 1995; Whelan 1996; Fouad and Pearson 1997; Pearson et al. 1998; Hiebert and Pearson 1999; Orlovsky et al. 1999; Lam and Pearson 2002; Frigon et al. 2010; Gottschall and Nichols 2011). Although the spinal reflexes continue to operate during locomotion, their pathways and relative contribution to motoneuronal activity during locomotion are modified. These modifications range from changes in reflex gain to complete reorganization of reflex pathways and emergence of new reflexes during locomotion (Pearson and Collins 1993; Guertin et al. 1995; McCrea et al. 1995; Pearson 1995; Perreault et al. 1995; Angel et al. 1996; Degtyarenko et al. 1998; Pearson et al. 1998; Burke 1999; Menard et al. 1999; Perreault et al. 1999; Gosgnach et al. 2000; Quevedo et al. 2000; Burke et al. 2001; McCrea 2001; Ross and Nichols 2009; Gottschall and Nichols 2011). An important finding has been that electrical stimulation of the group I extensor afferents enhances extensor activity if delivered during the extensor phase of locomotion and resets the rhythm to extension if delivered during the flexor phase (Conway et al. 1987; Guertin et al. 1995). In addition, the influence of the muscle force-sensitive group Ib afferents on ankle extensor activity is reversed from inhibition during non-locomotor conditions to excitation during locomotor activity (Pearson and Collins 1993; Gossard et al. 1994; McCrea et al. 1995), thus providing an additional mechanism for regulation of extensor activity depending on the load on the leg. However, the experiments in spinal cats trained to locomote on a treadmill have shown that these pathways cannot compensate for the total loss of cutaneous feedback from the paw (Bouyer and Rossignol 2003b). The length-dependent afferent feedback from the hip flexors is also important for control of stepping and is involved in the initiation of the swing phase and entrainment of locomotor activity (Andersson and Grillner 1983; Kriellaars et al. 1994; Hiebert et al. 1996; Lam and Pearson 2002).

Despite the significant amount of data on changes in locomotor activity produced by mechanical and electrical stimulations of muscles and neural circuits in the mammalian spinal cord, the structure and operation of spinal locomotor CPG(s) remain unknown (Grillner et al. 2008; McCrea and Rybak 2008; Gossard et al. 2011; Kiehn 2011; Yakovenko 2011; Guertin 2012). Computational models of the mammalian spinal circuitry and musculoskeletal system can complement experimental studies and propose explanations for the complex mechanisms of locomotor pattern generation. Several models of locomotor CPG have been developed based on data from so-called fictive locomotion generated within the spinal cord without afferent feedback from moving limbs (Cohen et al. 1982; Collins and Richmond 1994; Beer et al. 1999; Rybak et al. 2006a). However, as discussed above, afferent signals from moving limbs can reset the locomotor rhythm, advance or delay the phase transitions and modulate the duration of flexor and extensor phases. To understand the contribution of afferent feedback in locomotion, the computational models of spinal circuitries should include afferent feedback from the moving musculoskeletal system. Several such models have been developed and the possible mechanisms for sensory control of the CPG suggested (Taga 1995a, b; Wadden and Ekeberg 1998; Rybak et al. 2002; Ivashko et al. 2003; Ekeberg and Pearson 2005; Maufray et al. 2008; Aoi et al. 2013; Toth et al. 2013; Nassour et al. 2014); see also Chap. 8 in this book (Aoi 2015). Those models, however, have not attempted to reproduce the locomotor patterns of motoneuronal and afferent activity. Neither have they accurately reproduced the exact kinematics and kinetics of walking.

Our study has focused on the development of a comprehensive neuromechanical model of cat spinal locomotion. The neural subsystem of this model includes a locomotor CPG. The model of this CPG is based on the previously developed two-level model (Rybak et al. 2006a, b). The basic two-level CPG model included separate *rhythm generation* (RG) and *pattern formation* (PF) networks. This basic model has been extended to accommodate and reproduce the realistic activity patterns of motoneurons controlling complex two-joint muscles (see Chap. 5 by Shevtsova et al. 2015). In this study we connected the extended CPG model with the comprehensive hindlimb musculoskeletal model simulating biomechanics of cat walking and providing motion-dependent afferent feedback to the CPG (Prilutsky et al., Chap. 10, in this volume). The combined neuromechanical model demonstrates the ability to generate stable locomotion showing realistic patterns of muscle activity and mechanical characteristics of walking. The model has been used for the investigation of the role of particular afferent pathways for stable walking.

2.2 Musculoskeletal Model of Hindlimbs

The musculoskeletal model of the cat hindlimbs is described in details in Chap. 10 of this book (Prilutsky et al. 2015) and only its brief description is provided here. The two cat's hindlimbs, pelvis and trunk are modeled as a 2D, 10 degrees-of-freedom (DOF) system of rigid segments interconnected by frictionless revolute joints (Fig. 2.1a and b). Interactions of hindlimbs with the ground and the trunk with the forelimbs,

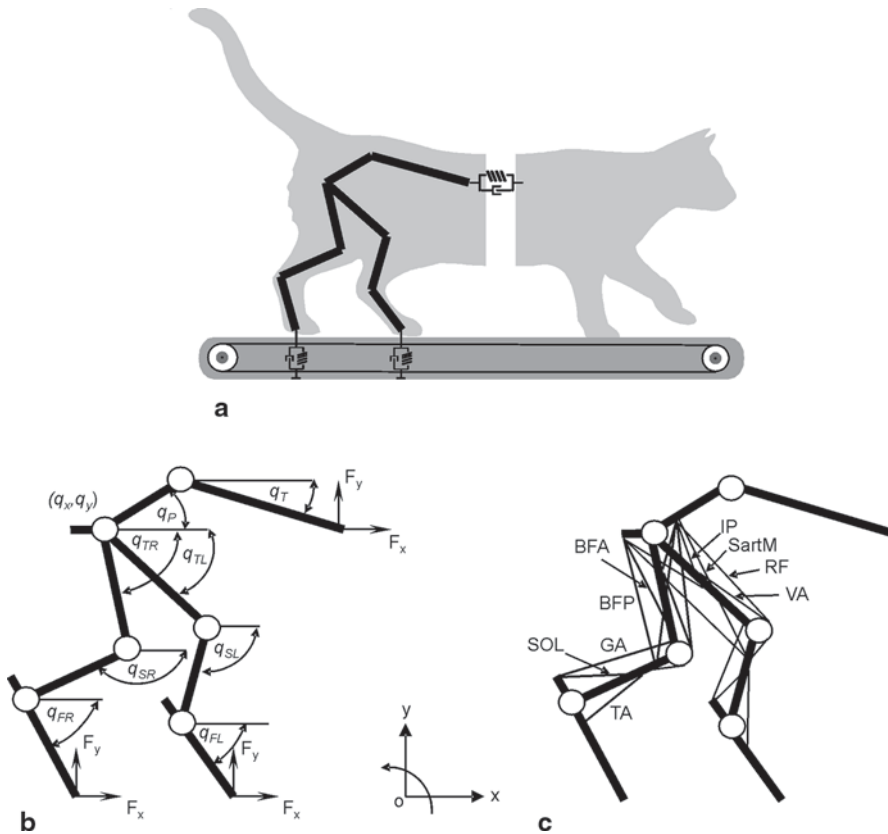


Fig. 2.1 Schematic representation of the musculoskeletal model of the cat hindlimbs and trunk. **a** The hindlimbs and posterior trunk interact with the ground and the anterior trunk and forelimbs. These interactions are modeled as viscoelastic forces. **b** A 10-DOF planar system of rigid segments with frictionless revolute joints representing two hindlimbs, pelvis and posterior trunk. **c** Schematic representation of muscles of the model: *IP* iliopsoas, *BFA* biceps femoris anterior, *RF* rectus femoris, *BFP* biceps femoris posterior, *SartM* sartorius medial, *VA* vastii, *GA* gastrocnemii, *TA* tibialis anterior, and *SOL* soleus. (Adopted from Prilutsky et al., Chap. 10, in this volume)

neck and head are modeled as linear springs with dampers. The inertial parameters of hindlimb segments are computed from the measured mass of the cat and length of each hindlimb segment using the regression equations (Hoy and Zernicke 1985). The equations of motion are derived from the Lagrange equations. The generalized coordinates of the model include the horizontal and vertical positions of the hip and the segment angles (Fig. 2.1b). The equations of hindlimbs dynamics include the vectors of segmental generalized velocities and accelerations, Coriolis and centrifugal forces, gravitational forces, ground and trunk reaction forces, muscle forces, and viscoelastic forces at the joints (for details see Prilutsky et al. 2015, Chap. 10, in this volume).

Each hindlimb in the model is actuated by 9 muscles described by Hill-type models (Fig. 2.1c) with realistic tendon force-length properties, contractile element force-length-velocity properties, muscle mass and angle of pennation as well as a parallel elastic component (Prilutsky et al. 2015; Chap. 10, in this volume). The

description of contractile and activation dynamics of the muscle-tendon actuator can be found in Chap. 10 of this volume (Prilutsky et al. 2015).

Parameters of the musculoskeletal model (constants for the viscoelastic elements producing reaction forces, the tendon slack length, tendon force-length relationship parameters, maximal muscle activation, activation and deactivation time constants for each muscle-tendon unit, etc.; see Prilutsky et al. 2015, Chap. 10, in this volume), were identified by minimizing the mismatch between the simulated and experimentally obtained cat locomotion variables—muscle fascicle lengths/velocities, joint angles, joint moments and ground reaction forces—using a parallel simulated annealing optimization algorithm (Corana et al. 1987). The simulated walking mechanics were obtained by integrating the equations of the limb and muscle dynamics, using the recorded activity of 9 muscles as input and the recorded position and velocity of each generalized hindlimb coordinate at the walking cycle onset as the initial conditions (Prilutsky et al. 2015, Chap. 10, in this volume). The obtained parameters of the musculoskeletal model were within physiological ranges reported in the literature (e.g., Spector et al. 1980; Sacks and Roy 1982; Baratta et al. 1993, 1995; Brown et al. 1996) and allowed for a close match (typically within one standard deviation) between the simulated and recorded joint angles and moments as well as ground reaction forces during walking.

The firing rates of spindle length-sensitive group Ia and II afferents and force-sensitive Golgi tendon organ group Ib afferents are closely correlated with the instantaneous muscle length/stretch velocity and tendon force, respectively, as observed during walking in the cat (Prochazka et al. 1997; Prochazka and Gorassini 1998). This fact makes it possible to estimate the firing rates of spindle and Golgi tendon organ afferents as functions of muscle fascicle length and velocity and tendon force of each muscle-tendon unit in the musculoskeletal model using equations similar to those proposed by Prochazka et al. (Prochazka and Gorassini 1998; Prochazka 1999). Another important afferent signal that indicates the stance phase of locomotion and influences the CPG operation and locomotor rhythm is activity of load-sensitive cutaneous afferents from the paw pad (McCrea 2001). The firing rate of these afferents is computed as the function of the ground reaction force and its time derivative (Prilutsky et al. 2015, Chap. 10, in this volume).

2.3 Model of Spinal Circuitry

2.3.1 Neuron Models

The model of the spinal circuitry in this study represents a modified version of the two-level locomotor CPG model described in Chap. 5 of this volume (Shevtsova et al. 2015). The model includes a bipartite (half-center) rhythm generator, pattern formation network and other interneurons and motoneurons. The interneurons provide basic reflex circuits including reciprocal inhibition of antagonistic motoneurons, recurrent inhibition of motoneurons via Renshaw cells, disynaptic excitation of some motoneuron types, etc. The CPG model of Shevtsova et al. 2015 (see Chap. 5)

was simplified so that each neuronal population was described by an activity-based (non-spiking) neuron model. Two types of neuron models were implemented: one for rhythm-generating RG and PF neurons and motoneurons and the other for all other neurons.

The membrane potentials (V) of principal neurons at RG, PF levels and motoneurons are described by the following equation:

$$C \cdot \frac{dV}{dt} = -I_{NaP} - I_K - I_{Leak} - I_{SynE} - I_{SynI} . \quad (2.1)$$

The membrane potential of all other neurons is described as:

$$C \cdot \frac{dV}{dt} = -I_{Leak} - I_{SynE} - I_{SynI} , \quad (2.2)$$

where C is the neuronal capacitance, I_{Leak} is the leakage current, I_K is potassium rectifier current, I_{NaP} is persistent sodium current; I_{SynE} and I_{SynI} are the excitatory and inhibitory synaptic currents, respectively. The ionic currents are described as follows:

$$\begin{aligned} I_{NaP} &= \bar{g}_{NaP} \cdot m_{NaP} \cdot h_{NaP} \cdot (V - E_{Na}); \\ I_K &= \bar{g}_K \cdot m_K^4 \cdot (V - E_K); \\ I_{Leak} &= \bar{g}_{Leak} \cdot (V - E_{Leak}); \\ I_{SynE,i} &= \bar{g}_{SynE} \cdot (V_i - E_{SynE}) \cdot \left(\sum_j a_{ji} \cdot f(V_j) + \sum c_{mi} \cdot d_m + \sum_k w_{ki} \cdot fb_k \right); \\ I_{SynI,i} &= \bar{g}_{SynI} \cdot (V_i - E_{SynI}) \cdot \sum_j b_{ji} \cdot f(V_j), \end{aligned} \quad (2.3)$$

where \bar{g}_{NaP} , \bar{g}_{Leak} , \bar{g}_{SynE} , and \bar{g}_{SynI} are the maximal conductances of the corresponding ionic channels; E_{Na} , E_K , E_L , E_{SynE} , and E_{SynI} are the corresponding reversal potentials; a_{ji} defines the weight of the excitatory synaptic input from neuron j to neuron i ; b_{ji} defines the weight of the inhibitory input from neuron j to neuron i ; c_{mi} defines the weight of the excitatory drive d_m to neuron i ; w_{ki} defines the synaptic weight of afferent feedback fb_k ($k=Ia, Ib, II$, cutaneous) to neuron i ; (see Tables 2.1, 2.2, 2.3, 2.4, 2.5, 2.6, 2.7, 2.8, and 2.9 in Appendix). Activation of the potassium delayed rectifier and persistent sodium currents is considered instantaneous. Voltage dependent activation and inactivation variables and time constant for the potassium delayed rectifier and persistent sodium channels are described as follows:

$$\begin{aligned} m_K &= 1 / (1 + \exp(-(V + 44.5) / 5)), \\ m_{NaP} &= 1 / (1 + \exp(-(V + 47.1) / 3.1)), \\ \tau_{hNaP} \cdot \frac{d}{dt} h_{NaP} &= h_{\infty NaP} - h_{NaP}, \\ h_{\infty NaP} &= 1 / (1 + \exp(-(V + 51) / 4)), \\ \tau_{hNaP} &= \tau_{hNaP \max} / \cosh((V + 51) / 8). \end{aligned} \quad (2.4)$$

The neuron output activity is defined by a nonlinear function $f(V)$:

$$f(V) = \begin{cases} 1 / (1 + \exp(-(V - V_{1/2}) / k)), & \text{if } V \geq V_{tr}; \\ 0, & \text{if } V < V_{tr}, \end{cases} \quad (2.5)$$

where $V_{1/2}$ is the half-activation voltage, k defines the slope of the output function and V_{tr} is the threshold.

The following values of neuronal parameters were used: $C = 20$ pF; $E_{Na} = 55$ mV, $E_K = -80$ mV, $E_{SynE} = -10$ mV, $E_{SynI} = -70$ mV, $E_{Leak} = -64$ mV for RG, PF neurons and motoneurons and -60 mV for all other neurons; $\bar{g}_K = 4.5$ nS, $\bar{g}_{Leak} = 1.60$ nS, $\bar{g}_{SynE} = \bar{g}_{SynI} = 10.0$ nS, $\bar{g}_{NaP} = 3.5$ nS for RG neurons, 0.5 nS for PF neurons, and 0.3 nS for motoneurons; $\tau_{hNaP} = 600$ ms. Parameters of $f(V)$ function were $V_{1/2} = -30$ mV, $V_{tr} = -50$ mV, $k = 3$ mV for motoneurons and 8 mV for other neurons.

The model of locomotor center (Fig. 2.2) incorporates the model of CPG and basic reflex circuits mediating the reciprocal inhibition of antagonistic motoneurons via Ia inhibitory interneurons, recurrent inhibition of motoneurons via Renshaw cells (RC), non-reciprocal motoneuron inhibition (Ib cells) and disynaptic excitation of extensor motoneurons (Ia and Ib cells) (Fig. 2.3).

The conceptual architecture of the CPG model is based on the idea of a two-level locomotor CPG (Rybak et al. 2006a, b; McCrea and Rybak 2007, 2008). According to this hypothesis, the locomotor CPG consists of a half-center rhythm generator and multiple pattern formation circuits controlling different synergist and antagonist motoneuron pools (see Figs. 2.2 and 2.3). Depending on the input from the RG and the interactions within the PF network, each PF neuron is active within the particular phase(s) of the locomotor cycle and produces a phase-specific activity pattern. The specific principal PF elements control the corresponding group of synergistic motoneurons that are active synchronously. Organization of multiple neural circuits that control the activation of synergistic motoneuron groups is mainly unknown. Previous analysis based on the onset and offset times in motoneuron/muscle activity allowed to identify several synergistic groups of motoneurons operating during locomotion (Markin et al. 2012). The identified groups (see Fig. 2.4) include hip flexors (IP, SartM), hip extensor (BFA), knee extensor (VA), ankle flexor (TA), ankle extensors (GA, SOL), and two two-joint muscles BFP and RF, which demonstrate activity in both swing and stance phases. Figure 2.5 shows the proposed organization of rhythm generator and pattern formation circuits in the CPG controlling one hindlimb. All PF circuits receive excitatory and inhibitory inputs from rhythm generator and control flexor and extensor motoneurons operating at hip, knee and ankle as well as motoneurons controlling two-joint muscles (BFP, RF). Each joint-related PF circuitry is a half-center network consisting of PF-F and PF-E neurons reciprocally inhibiting each other via Inpf-F and Inpf-E inhibitory interneurons, respectively. The detailing description of PF organization can be found in Chap. 5 of this volume (Shevtsova et al. 2015).

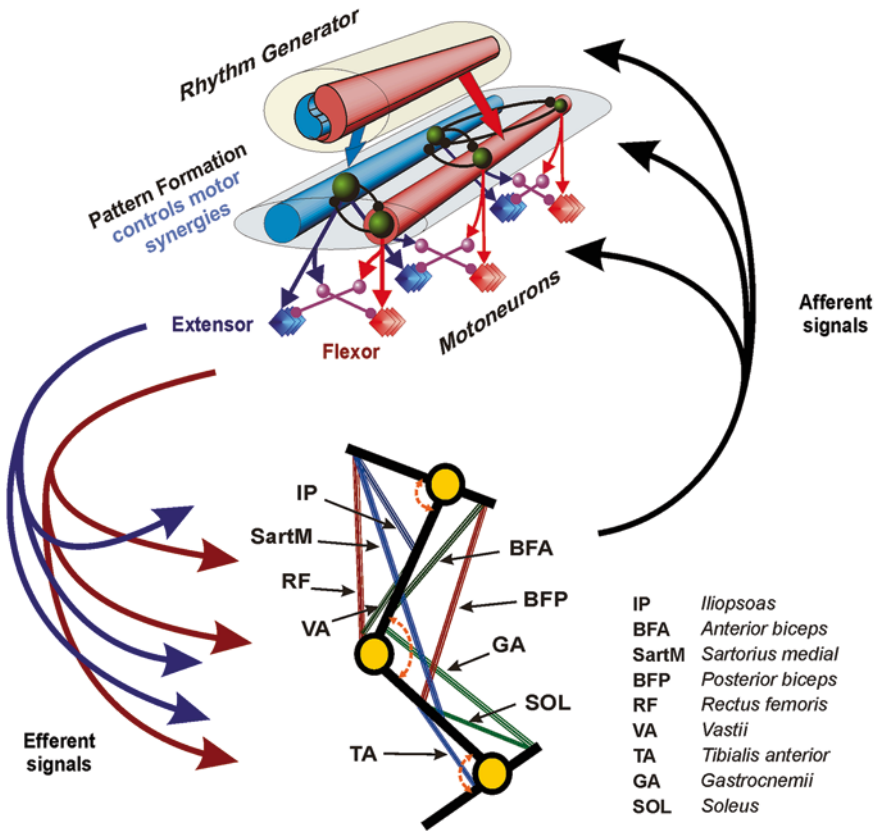


Fig. 2.2 General schematics of the neuromechanical model of the cat hindlimb locomotor control. The neural part of the model consists of the two-level locomotor CPG that controls the hindlimb musculoskeletal model. The activity of corresponding motoneuron pools controls major hindlimb muscles that drive the 10-DOF cat hindlimb model. The generated somatosensory feedback signals from the moving musculoskeletal hindlimb model (i.e., firing rates of group I and II muscle and paw pad cutaneous afferents) project onto both levels of the CPG (*RG* rhythm generator and *PF* pattern formation) and motoneuron level as well

2.4 Control of CPG by Afferent Feedback

Although the locomotor CPG can generate rhythm in the absence of sensory feedback signals, the sensory feedback plays a critical role in regulating phase transitions, stabilizing locomotor movements, contributing to weight support during the stance phase, and adjusting the locomotor pattern to the constantly changing external environment. A possible organization of afferent pathways to the CPG for a simple 1-DOF musculoskeletal system has been recently proposed (Markin et al. 2010). According to this organization, the stance-swing (extensor-flexor) phase transition was controlled by both the reduction of force-dependent afferent activity from the

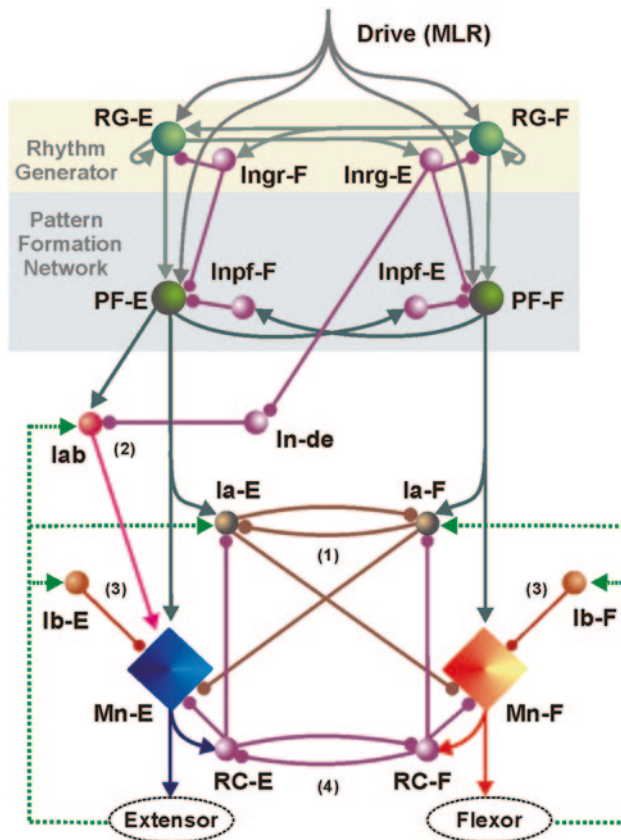


Fig. 2.3 Basic model of the two-level locomotor CPG model by (Rybak et al. 2006a, b) including reflex circuits: 1 reciprocal inhibition of antagonistic motoneurons via Ia inhibitory interneurons (*Ia-E* and *Ia-F*, correspondingly), 2 disynaptic excitation of extensor muscle motoneurons via *Iab* interneurons, 3 non-reciprocal inhibition of motoneurons via *Ib* inhibitory interneurons, and 4 recurrent inhibition via Renshaw cells (*RC-E* and *RC-F*, respectively)

extensor muscles and the increase in length-dependent afferent activity from the flexor muscles. Because of this organization, the duration of the stance phase depended on the locomotor speed. In contrast, the timing of the swing-stance (flexor-extensor) phase transition was mainly controlled by the length/velocity-dependent afferent activity from the hip extensor muscles; this feedback signal adjusted the duration of the flexor phase to limb kinematics during the swing phase, keeping the swing duration relatively constant.

In the present, more realistic neuromechanical model we have adopted the organization of sensory pathways between muscle afferents and RG-interneurons from the previous work (Markin et al. 2010). The type and organization of afferent pathways from the moving musculoskeletal system to the CPG have been chosen based

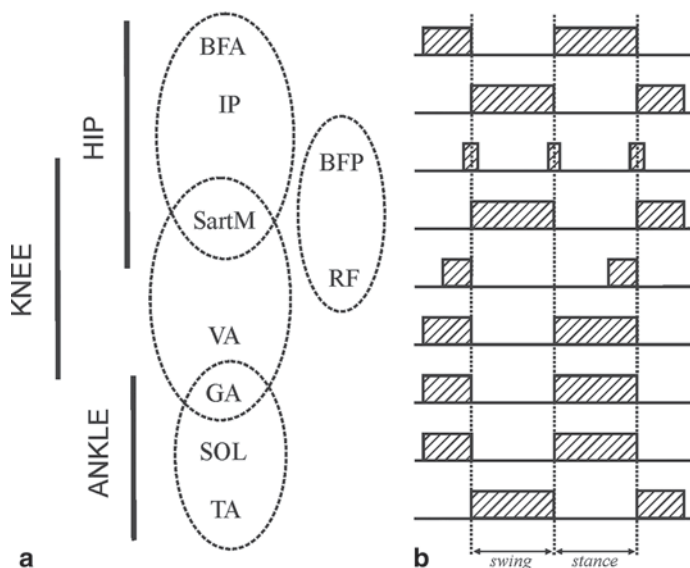


Fig. 2.4 Phases of activity of cat hindlimb muscles during real locomotion. **a** The possible organization of synergist motoneuron groups at the pattern formation level. Three circuits at the pattern formation level (hip-PF, knee-PF and ankle-PF) are introduced to control motoneuron groups innervating joint specific muscles: (1) BFA, IP, SartM as hip muscles; (2) VA, SartM, GA as knee muscles; and (3) GA, SOL, TA as ankle muscles. Note that two two-joint muscles (SartM and GA) receive control signal from hip-PF/knee-PF and knee-PF/ankle-PF sub-networks, respectively. The fourth circuit at pattern formation level specifically controls BFP and RF muscles that are partially active during both flexor and extensor phases. **b** Schematic representation of periods of EMG activity during level walking in the cat. While most of the hindlimb muscles are active during most of swing (flexor) or stance (extensor) phases, the two-joint BFP and RF muscles are only active at the swing-stance or stance-swing phase transition (BFP) or in the later part of the stance phase (RF)

on the following experimental data: (1) muscle length-sensitive spindle afferents of hip extensor and flexor muscles influence the flexor-extensor and extensor-flexor phase transitions (Perreault et al. 1995; Lam and Pearson 2002; McVea et al. 2005); and (2) activation of both group I and II afferents of ankle flexors can terminate flexor and initiate extensor phases during fictive locomotion (Perreault et al. 1995; Stecina et al. 2005); (3) group Ib afferents from the Golgi tendons organs of ankle extensors are responsible for prolongation of the stance phase (Duysens and Pearson 1980; Pearson 2008); (4) stimulation of cutaneous afferents innervating the paw pad can prolong the stance phase and is responsible for terminating the ongoing swing and initiating the stance phase (McCrea 2001; Rossignol et al. 2006). A possible organization of afferent signals at the RG-level for the CPG model is presented in Fig. 2.6. Two additional interneurons (Frg-F and Frg-E) are incorporated into the CPG model. These neurons receive the multi-modal afferent input signals from the afferents listed above and project their excitatory activity onto the corresponding neurons at the RG level.

Neuromechanical Modeling of Posture and Locomotion

Prilutsky, B.I.; Edwards, D.H. (Eds.)

2016, XI, 368 p. 116 illus., 52 illus. in color., Hardcover

ISBN: 978-1-4939-3266-5